THE BEHAVIOUR OF THE LSPMSM IN ASYNCHRONOUS OPERATION

Dan STOIA[1], Ovidiu CHIRILĂ[1], Mihai CERNAT[1], Kay HAMEYER[2], Drago BAN[3]

[1]"Transilvania" University of Brasov, Faculty of Electrical Engineering and Computer Sciences
B-dul Eroilor 29, 500036 Brasov, Romania, m.cernat@unitbv.ro

[2]RWTH Aachen University, Institute for Electrical Machines
Schinkelstraße 4, 52062 Aachen, Germany, kay.hameyer@iem.rwth-aachen.de

[3]University of Zagreb, Faculty of Electrical Engineering & Computing
Unska 3, 10000 Zagreb, Croatia, drago.ban@fer.hr

Abstract — The paper proposes a study of synchronization capability of line-start permanent magnet synchronous motor with small saliency ratio and very high cage resistance. The exemplified method is for a motor with the rated power of* 3.5 kW*, the synchronous speed of* 3000 rpm*, and the saliency ratio of* 1.08*.

Key words: AC machine, Permanent magnet motor, Synchronous motor, Design, Simulation, Efficiency, Power factor correction.

LIST OF NOTATIONS

- b_{M0} - no-load leakage flux coefficient of PM;
- b_{0s} - stator slot opening;
- B_{sy} - stator yoke flux density (average value);
- B_{rem} - remanent flux density of PMs;
- B_{δ} - air gap flux density (average value);
- $B_{\delta 0}$ - no-load air gap flux density (average value);
- C_p - permeance coefficient;
- C_{Φ} - magnetic flux concentration factor;
- $\underline{D}_C$ - cage damping factor (complex magnitude);
- D_M - PMs damping factor (real magnitude);
- D_{sin} - inner stator diameter;
- f_s - stator electrical frequency;
- f_t - frequency of the tooth ripple flux;
- h_2 - rotor tooth high;
- h_{sy} - effective high of the stator yoke;
- H_c - coercive magnetic field intensity;
- $\underline{I}_s$ - stator current;
- $\underline{I'}_D$ - rotor cage current related to the stator;
- I_M - stator current produced by the PMs;
- J - moment of inertia;
- k_C - Carter's coefficient;
- k_{Fe} - stator lamination stack coefficient;
- k_{sat} - saturation coefficient;
- $k^{(1)}_{ws}$ - fundamental stator winding factor;
- $k_{\sigma M}$ - leakage flux coefficient of PMs;
- l_{aM} - length of PMs in axial direction;
- l_{Fe} - stator lamination stack length in axial direction;
- l_M - length of PMs in magnetizing direction;
- N_D - number of rotor slots;
- N_s - number of stator slots;
- p - number of pole pairs;
- R_s - stator winding resistance;
- R_B - cage bar resistance;
- R_D - rotor (damper) resistance;
- R'_D - rotor resistance related to the stator;
- R_{Dd}, R_{Dq} - rotor resistance in *d-q* frame;
- R_{er} - resistance of end rings;
- s - slip between the stator rotating field and the rotor ;
- s_0 - slip value of start synchronizing process;
- s_{Kb} - critical slip value of the breaking torque;
- s_{KC} - critical slip value of the cage torque;
- t_B - barrier width;
- t_s - stator teeth width;
- T - electromagnetic torque;
- T_L - load torque;
- T_C - cage non-pulsating torque;
- T_M - non-pulsating (breaking) torque produced by PMs;
- T_p - pulsating torque;
- T_{pC} - pulsating component of the cage torque;
- T_{pM} - pulsating component of the magnet torque;
- U - supplying voltage, rms. value;
- U_{e0} - back EMF, rms. value;
- w_s - stator phase winding number;
- X_d, X_q - synchronous reactance in *d-q* frame;
- $X'_{D\sigma}$ - rotor leakage reactance related to the stator;
- X_m - main reactance;
- $X_{s\sigma}$ - stator leakage reactance;
- Z - input impedance;
- α_M - PM pole coverage;
- δ - air gap length
- Λ_M - permeance of PMs;
- Λ_r - permeance of the rotor teeth and of PM flux barriers;
- Λ_{δ} - air gap permeance;
- μ_0 - vacuum permeability;
- μ_{rec} - recoil relative permeability of PM;
- τ_p - pole pitch;
- ξ - saliency ratio;
- ω_C - cage angular frequency;
- ω_s - stator angular frequency;

I. INTRODUCTION

The line-start permanent magnet synchronous motor (LSPMSM) represents an interesting, energy saving and high efficient alternative for asynchronous motors, used in low-cost electric drives, where the usage of current controlled voltage source inverters is too expensive. Even, in these simple drives, the design considering the dynamic behaviour is important, because every good line-start motor has to be able to synchronize under load after line-starting.

For asynchronous line starting, the rotor contains an aluminium cage, which plays a role during the transient processes. For amplifying the saliency, the rotor contains magnetic flux barriers on its direct axis and non-magnetic flux barriers on its quadrate axis, last ones used also

978-1-4244-7855-2/10/$26.00 ©2010 IEEE

for minimizing the inter-pole PM leakage flux. The PMs inserted as magnetic flux barriers are located in the rotor back iron, bellow the squirrel-cage. The stator structure is the same as that of an ordinary induction machine.

In order to evaluate the LSPMSM's line starting performances, when coupled at different loads and fed by different supply voltages, a reliably dynamic model of the motor is required because its line-starting and synchronization capabilities depend on various design parameters (e.g. squirrel cage design and material, design of magnetic flux barriers, placement of PMs, etc.[2, 4, 5, 7, 10-13, 16]).

The paper presents a study of the synchronization capability of LSPMSMs with small saliency ratio and very high cage resistance. The behaviour of LSPMSM in asynchronous operation is exemplified for a motor with the rated power of 3.5 kW, the synchronous speed of 3000 rpm, the saliency ratio of 1.08 and the rotor resistance, R'_D, of 0.055 p.u..

II. THE MAIN DESIGN PARAMETERS

The line-start is properly obtained thanks of the rotor design. Due to manufacturing reasons, rotor closed slots are preferred by mainly producers. If a die casting process is applied on the rotor manufacturing, the closed rotor slots prevent the cast from spilling outside the rotor. It must be noted, however the iron bridge above the rotor slots is made very thin, and that means this is heavily saturated even on normal operation. In Fig. 1 a rotor cross section of our machine is shown.

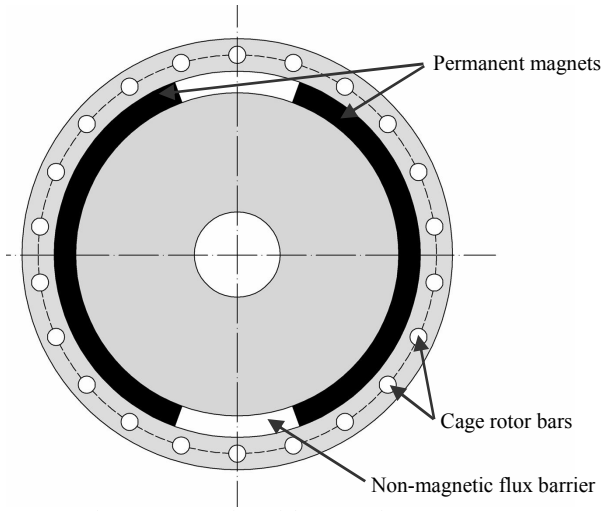

Fig. 1. Cross section of the rotor of a LSPMSM [18].

The components of the torque may be calculated from individual equivalent circuits: one for the induction motor and other for the PM generator [6, 7].

For reducing the space occupied by PMs and making sure that the power density is enough high, sintered NdBFe magnets are used.

The PM volume mainly relies on the following factors:

- the operating point of PMs;
- the maximal energy produced by the PMs;
- the back EMF;
- the leakage coefficient;
- the magnetic saturation coefficient.

The PM dimensions may be determined and optimized by a combined graphical and analytical method in order to obtain the no-load voltage to choose as input design parameter [1, 3].

According to the imposed magnetic energy curve of PMs and the very little space between the PM and squirrel cage (because of the position of PM into the rotor), the expected energy utilization ratio could be estimated through the operating point of PM in the rotor magnetic circuit [1, 17]:

$$C_p = \mu_{rec} \frac{\Lambda_\delta + \Lambda_r}{\Lambda_M} \tag{1}$$

where the permeances are expressed by:

$$\Lambda_\delta = \mu_0 \frac{\alpha_M \ \tau_p \ l_{\mathrm{Fe}}}{2\,\delta\,k_C} \tag{2}$$

$$\Lambda_r = \mu_0 \ \mu_{rec} \frac{\alpha_M \ t_B \ l_{\mathrm{Fe}}}{2\ h_2} \tag{3}$$

$$\Lambda_M = \mu_0 \ \mu_{rec} B_{rem} / H_c \tag{4}$$

By taking into account the magnetic saturation of the iron, the air gap flux density at no-load operation can be expressed as [1],

$$B_{\delta 0} = \frac{C_\Phi}{1 + \mu_{rec} \dfrac{k_C \ k_{\sigma M} \ k_{sat}}{C_p}} B_{rem} \tag{5}$$

$$C_\Phi = 2\,\alpha_M / \left(1 + \alpha_M\right) \tag{6}$$

$$k_{\sigma M} = 1 + \frac{4\,l_M}{\pi\,\mu_{rec}\ \alpha_M\ \tau_p} \ln\left[1 + \frac{\pi\,\delta}{(1-\alpha_M)\,\tau_p}\right] \tag{7}$$

$$k_C = t_s / \left(\ t_s - \gamma_s\ \delta\right) \tag{8}$$

$$\gamma_s = \frac{4}{\pi}\left[\left(\frac{b_{0s}}{2\,\delta}\right)\tan^{-1}\left(\frac{b_{0s}}{2\,\delta}\right) - \ln\sqrt{1+\left(\frac{b_{0s}}{2\,\delta}\right)^2}\right] \tag{9}$$

It is to note that the leakage coefficient of PM $k_{\sigma M}$ and the performances of the motor are influenced by the size of PMs, which becomes a very important parameter of the machine.

For the sizing procedure, the air-gap flux density can be initially estimated as

$$b_{M0} = \frac{B_{\delta 0}}{B_{rem}} = 0.75 - 0.9 \tag{10}$$

and during this sizing procedure the coverage coefficient α_M and the leakage flux coefficient of PM b_{M0} will be determined by iteration taking into the magnetizing curve and maximizing the density of the magnetic energy of the PM [1].

The length of the PM in the magnetizing direction results [1]:

$$l_M = 2\,\delta\,b_{M0} / \left(1 - b_{M0}\right) \tag{11}$$

In this way, the back EMF can be expressed as [1]:

$$U_{e0} = 4.44 f\, k_{ws}^{(1)} w_s \frac{b_{M0}\, B_{rem}\, \tau_p\, \alpha_M\, l_{\mathrm{Fe}}}{k_{\sigma M}} \qquad (12)$$

and it is direct proportional to the remanent flux density of PMs. The value of B_{rem} depends on the producer and of the temperature, too. So, the value of the back EMF depends of the armature winding temperature.

The effective high of the stator yoke can be iteratively obtained from the following equation [7]:

$$h_{sy} = \frac{\pi\, D_{sin}\, \alpha_M\, B_\delta}{4\, p\, k_{\mathrm{Fe}} B_{sy}} \qquad (13)$$

For machines with a small number of poles pairs, the height and the length (the radial and axial dimensions) of the stator yoke are small and the magnetic flux density is high, but it have to be limited to 1.8 T.

The design of the squirrel cage mainly contains the selection of slot number and the dimensioning. The squirrel cage influence on the starting ability of the motor depends on the slot number and on the cage resistance.

The influence of the eddy currents in rotor ends of the skin effect into the cage end rings is taken into account by the coefficient k_{sk}, introduced as follows.

For bars which are equal distributed on the rotor circumference, the equivalent resistance of the rotor bars including the rotor end rings can be expressed by [7]:

$$R_D = R_B + R_{er} \frac{N_D}{(2\, p\, \pi)^2} \qquad (14)$$

For taking into account the rotor bar current influence of the fundamental space harmonic of the air-gap magnetic flux density, a coefficient named k_{sk} was introduced:

$$k_{sk} = R_B / R_D \qquad (15)$$

III. The Torques of the LSPMSM in Asynchronous Operation

During asynchronous operation the run-up torque comprises basically two components, one the non-pulsating component that comprises cage component T_C, and PM component T_M, and other, the pulsating component that comprises PM pulsating component T_{pM} with the frequency $s f_s$, arising from the interaction between magnet flux and rotor cage current [13, 16] and cage pulsating component T_{pC} [9].

The non-pulsating cage torque T_C has two principal oscillating components, one has the frequency $2 s f_s$ due to the mechanical reluctance variation, and the other has the frequency $s f_s$ due to the magnetic saturation. The variation of reluctance caused by the rotor geometry generates a reluctance torque and an asynchronous starting torque that pulsate with the frequency $2 s f_s$ during asynchronous operation. The magnetic saturation, which is caused by the PM flux, generates another collateral reluctance variation which result is a pulsation with the frequency $s f_s$. This special torque pulsation appears only in the LSPMSM.

So, in asynchronous period, the torques are given by:

$$T = T_{av} + T_p; \quad T_P = T_{pM} + T_{pC}; \quad T_{av} = T_C + T_M \qquad (16)$$

During the design stage, for optimizing the starting torque characteristic, a separate treatment of the two torque components, the driving asynchronous cage torque and the braking magnet torques, is helpful.

The torque of induction motor can be derived from the common simplified equivalent circuit of an induction motor shown in Fig. 2.

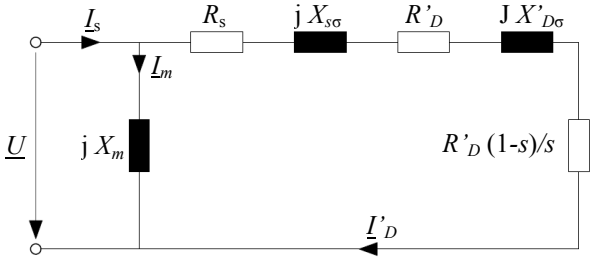

Fig. 2. Simplified equivalent circuit of an induction motor

In this way, from the basic equations expressed in *d-q* reference frame, it can be expressed a few mainly parameters which affect the sensitivity of the synchronization capability [8, 13, 14, 15, 17, 18].

Thus, the rotor cage reaction on the primary field can be defined by the complex field damping factor:

$$\underline{D}_C = \frac{R'_D + \mathrm{j}\, s\, X'_{D\sigma}}{R'_D + \mathrm{j}\, s\, (X_m + X'_{D\sigma})} \qquad (17)$$

The stator winding resistance R_s is an important parameter in the asynchronous operation. The average torque T_{av} which amplifies the half synchronous speed „dips“ can be minimized by using a minimum admissible value for the stator resistance.

The input equivalent impedance is:

$$\underline{Z} = R_s + \mathrm{j}\, X_{s\sigma} + \mathrm{j}\, X_m\, \underline{D}_C \qquad (18)$$

From the equivalent scheme (Fig. 1) it can be deduced:

$$-\underline{I}'_D = \underline{I}_s \frac{\mathrm{j}\, X_m\, \underline{D}_C}{\frac{R'_D}{s} + \mathrm{j}\, X_m\, \underline{D}_C} \qquad (19)$$

and the rotor current I'_D can be expressed as,

$$I'_D = \frac{U}{\sqrt{\left(R_s + R'_D/s\right)^2 + \left(\omega_s L_{s\sigma} + \omega_s L'_{D\sigma}\right)^2}} \qquad (20)$$

The cage non-pulsating torque is given by:

$$T_C = \frac{3p}{\omega_s} \frac{\frac{R'_D}{s} U^2}{\left(R_s + R'_D/s\right)^2 + \left(\omega_s L_{s\sigma} + \omega_s L'_{D\sigma}\right)^2} \qquad (21)$$

The maximum value for the cage torque is given, when the derivative of above equation (21), with respect R'_D/s is set to zero and the critical slip value (the pull-out slip)

for this torque is given by:

$$s_{KC} = \frac{R'_D}{\sqrt{R_s^2 + \omega_s^2 \left(L_{s\sigma} + L'_{D\sigma}\right)^2}} \tag{22}$$

By above equations, an equation for the pull-out torque can be written as:

$$T_{KC} = \frac{3p}{2\omega_s} \frac{U^2}{R_s + \sqrt{R_s^2 + \omega_s^2 \left(L_{s\sigma} + L'_{D\sigma}\right)^2}} \tag{23}$$

Using the equivalent circuit of the induction motor with closed rotor slots, the current magnitude during the starting sequence can be derived and the line current magnitude is

$$\left| \underline{I}_s \right| = \left| \underline{I}'_D + \underline{I}_m \right| \tag{24}$$

where $\underline{I}'_D$ and I_m are the rotor and magnetizing branch currents (Fig. 1).

Fig. 3 shows the simplified equivalent circuit of a PM generator which allows the computation of the braking torque produced by the permanent magnet.

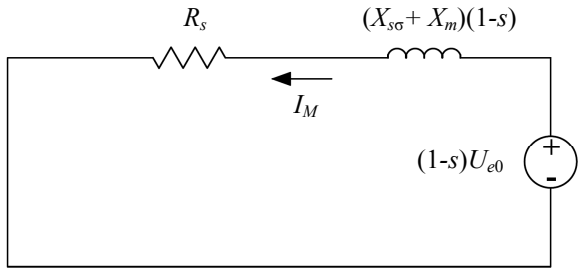

Fig. 3. Simplified equivalent circuit of a PM generator.

The flux of the PMs produces the current I_M in the stator winding [1]

$$I_M = -(1-s)^2 X_q \, U_{e0} / D_M \tag{25}$$

where

$$D_M = R_s^2 + (1-s)^2 X_m^2; \quad X_m = \left(X_{ad} + X_{aq}\right)/2 \tag{26}$$

and will cause the breaking torque:

$$T_M = -\frac{3p}{\omega_s} R_s \, I_M^2 \tag{27}$$

The critical slip value for obtaining the maximum breaking torque is:

$$s_{Kb} = 1 - \zeta \sqrt{1.5\,(\xi - 1) + \sqrt{1.5\,(\xi - 1)^2 + \xi}} \tag{28}$$

$$\xi = X_q / X_d; \qquad \zeta = R_s / X_d \tag{29a, b}$$

IV. STARTING PROCESS ANALISYS

The exemplified method is for a motor with the rated power of 3.5 kW, the synchronous speed of 3000 rpm, and the saliency ratio of 1.08. The values of principal parameters were: U_N = 108 V; U_{e0} = 100 V; R_s = 0.27 Ω; R'_D = 0.27 Ω; $X_{S\sigma}$ = 0.198 Ω; $X_{D\sigma}$ = 0.198 Ω; X_d = 2.28 Ω; X_q = 2.46 Ω; X_m = 2.17 Ω. The analysis is making for an initial internal angle equal with 30 electrical grades.

By analysing Fig. 4, Fig. 5 and Fig. 6 the starting process can be approximately divided into three stages:

a) *The accelerating process*: the rotor accelerates from standstill. The instantaneous rotor acceleration is given (neglecting the friction torque) by:

$$ps\omega_s = \frac{p}{2J}(T_{av} - T_L) \tag{30}$$

The rated starting time constant of the motor is τ_j = 400 ms. The peak value of the a phase inrush current is 6.55 I_N. As shown in Fig. 4, during acceleration process, the average cage torque is positive and contributes to rotor acceleration, while the average magnet torque is negative acts as a brake. Pulsating, the magnet and the cage torque, seem to be subject to the slip frequency. The pulsating torque with frequency 2 $s f_s$ can not be seen in the cage torque due to the small saliency. In this stage will present the classical „dip“ at half synchronous speed, in a similar way to the Georges phenomenon in induction motors unsymmetrical rotor. This „dip“ can be minimized by using symmetrical cage rotors (i.e. $R_{Dd} \approx R_{Dq}$). In this stage the rotor higher resistance has a beneficial effect an early start (i.e. $R'_D \sim s_{KC}$ and $R'_D \sim T_{em}$). In this period the brake reluctance torque due to the saliency is very small.

b) *Pulling into the synchronization period*: in this stage the average torque attains the zero value corresponding to an initial slip s_0 proper pull in synchronization period. Higher resistance rotor increases the slip at which the synchronization occurs, s_0. Therefore more energy is needed to synchronize the motor. If the average torque decreases the rotor tries to pull-out in under the influence of the average and pulsating magnet torques components which acts as steady state in this stage. Thus the rotor is accelerated up to the synchronous speed mainly by the magnet torque, while the cage torque generates a little negative and positive rotating torque alternatively. As the synchronous torque increases only proportionally to the back EMF, it happens that the increase of synchronizing energy is compensated for a value of the back EMF (the no-load voltage) which maximizes the critical load torque.

c) *Synchronous operation period*: in this stage the motor goes into damped oscillation procedure around a slip s_0, when the rotor cage currents tend to be amortized (see Fig. 6) and the damping of oscillation, proportion with the back EMF, is small and this period of synchronization is relatively long.

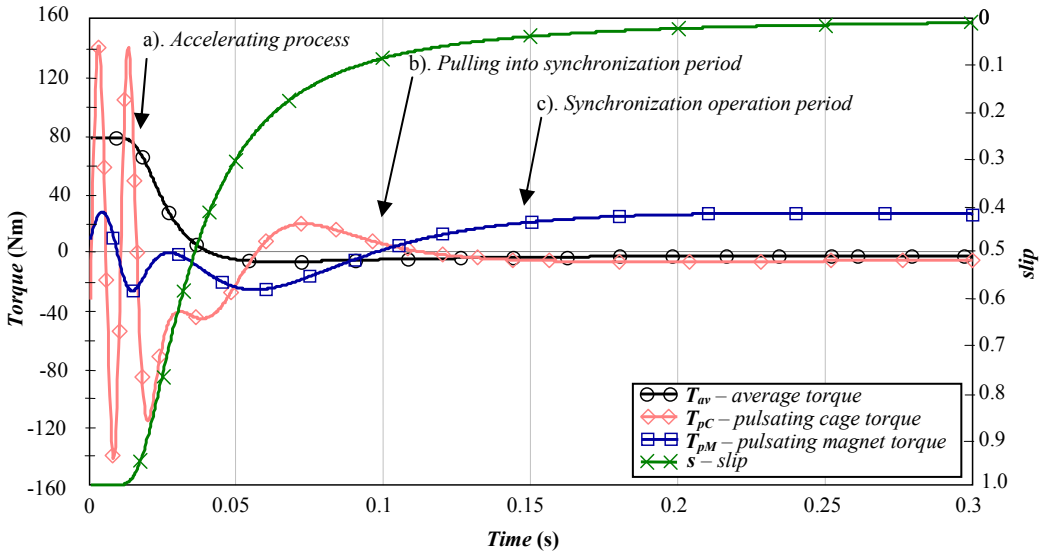

Fig. 4. Average torque, pulsating cage torque, pulsating magnet torque and slip versus time.

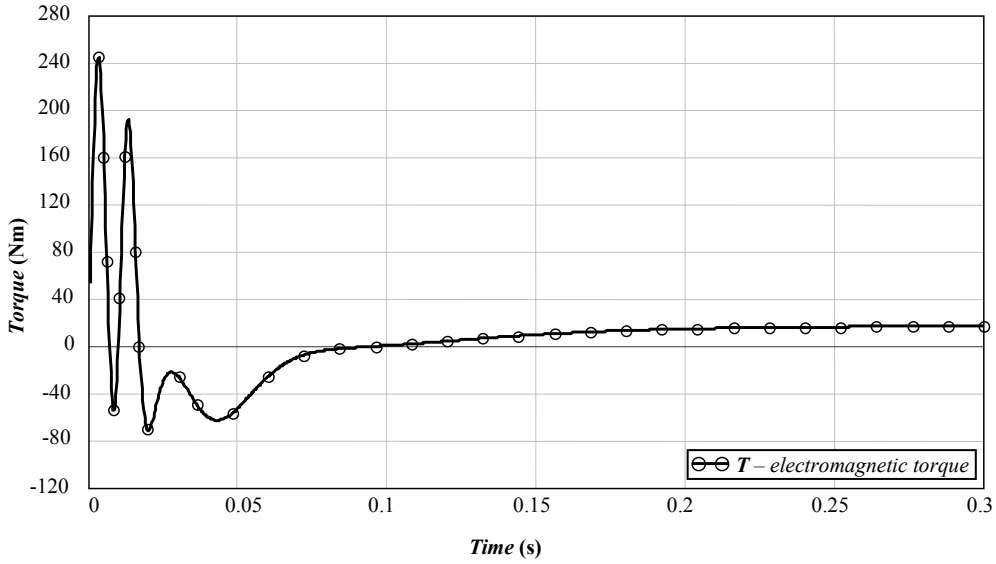

Fig. 5. Electromagnetic torque versus time.

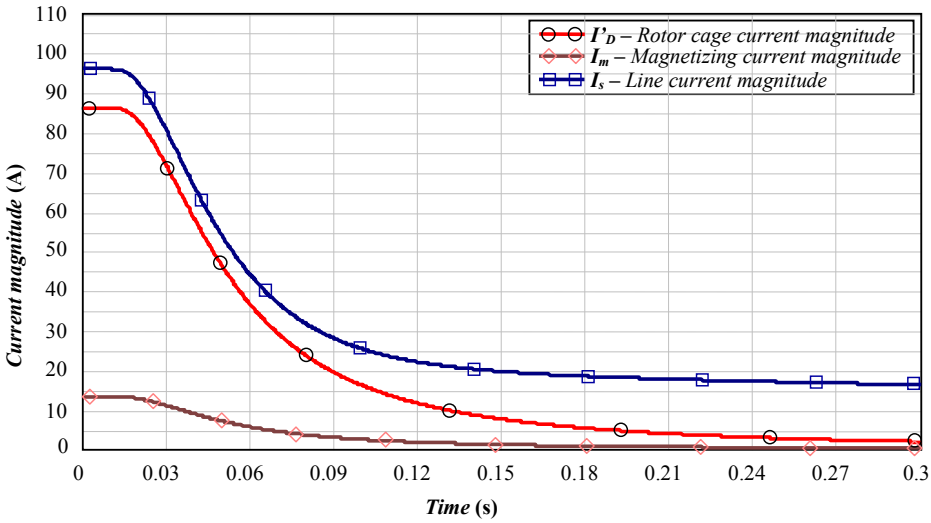

Fig. 6. Currents during starting process versus time.

CONCLUSIONS

The paper has proposed a study of synchronization capability of LSPMSM with very high cage resistance and small saliency ratio. The high value of the rotor resistance of the designed motor has beneficial effects on the early start, but the synchronization occurs at a large value of the slip and is relatively difficult. A minimal optimum value of synchronization energy has been found for the no-load voltage which maximizes the critical electromagnetic torque. For a better synchronization capability, it has used a permanent magnet with low volume.

The calculated value if the back EMF (the no-load voltage) is low; the value of magnetization inductance is relatively big. So, more energy for synchronization is available, but the motor has a reduced overcharge capability.

REFERENCES

[1] D. Stoia, M. Cernat, "Design of Line-Start Permanent Magnet Synchronous Motors," *ICIE 2009,* Vilnius, Lituania, May 2009.

[2] E. Peralta-Sanchez and A.C. Smith, "Line-start permanent-magnet machines using a canned rotor," *IEMDC 2007*, Antalya, Turkey, vol. 2, pp. 1084-1089, May 2007.

[3] G. Yang, J. Ma, J.X. Shen, and Y. Wang, "Optimal Design and Experimental Verification of a Line-Start Permanent Magnet Synchronous Motor," *ICEMS 2008*, Wuhan, China, pp. 3232 - 3236, Oct. 2008.

[4] H. Nam, S.B. Park, G.H. Kang, J.P. Hong, J.B. Eom, and T.U. Jung, "Design to Improve Starting Performance of Line-Start Synchronous Reluctance Motor for Household Appliances," *IEEE IAS Ann. Meet. 2004*, Seatle, USA, pp.79-85, Oct. 2004.

[5] J. Salo, T. Heikkila, J. Pyrhonen, "New low-speed high-torque permanent magnet synchronous machine with buried magnets," *ICEM 2000,* Espoo, Finland, vol.2, pp.1246-1250, Aug. 2000.

[6] J. Soulard and H.P. Nee, "Study of the synchronization of line-start permanent magnet synchronous motors," *IEEE IAS Annual Meeting 2008*, Edmonton, Alberta, Canada, vol. 1, pp. 424-431, Oct. 2008.

[7] K. Kurihara and A. Rahman, "High-efficiency line-start interior permanent-magnet synchronous motors," *IEEE Trans. Ind. Appl.*, vol. 40, no. 3, pp. 789-796, May/Jun. 2004.

[8] I. Tsuboi, I. Hirotsuka, T. Takegami, and M. Nakamura, "Basic Concept of an Analytical Calculation Method and Some Test Results for Determination of Constant of Line Start Permanent Magnet Motor," *ICEMS 2008*, Wuhan, China, pp. 3108-3111, Oct. 2008.

[9] M. Popescu, T.J.E. Miller, M. McGilp, D.M. Ionel, S.J. Dellinger, "A Unified Approach to the Synchronous Performance Analysis of Single and Poly-Phase Line-Fed Interior Permanent Magnet Motors," *IEEE IAS Annual Meeting 2007*, New Orleans, Louisiana, USA, pp. 148 - 153, Sept. 2007.

[10] Q.F. Lu and Y.Y. Ye, "Design and Analysis of Large Capacity Line-Start Permanent-Magnet Motor," *IEEE Trans. Magnetics*, Vol. 44, No. 11, Nov. 2008, pp 4417-4420.

[11] W.H. Kim, K.C. Kim, S.J. Kim, et al., "A Study on the Optimal Rotor Design of LSPM Considering the Starting Torque and Efficiency," *IEEE Trans. Magnetics*, Vol. 45, No. 3, March 2009, pp. 1808-1811.

[12] Z. Bingyi, Z. Wei, Z. Fuyu, F. Guihong, "Design and Starting Process Analysis of Multipolar Line-Start PMSM," *Proc. ICEMS 2007*, Seoul, Koreea, pp. 1629-1634, Oct. 2007.

[13] V.B. Honsinger, "Permanent Magnet Machines: Asynchronous Operation," *IEEE*, Vol. PAS-99, No. 4 July/Aug 1980, pp. 1503-1509.

[14] B. Zhang, W. Zhang, F. Zhuang, G. Feng, "Design and Starting Process Analysis of Multipolar Line-Start PMSM," *Proc. ICEMS 2007*, Seoul, Korea, pp 1629-1634, Oct. 2007.

[15] A. Abbas, H.A. Yousef, O.A. Sebakhy, "FE Parameters Sensitivity Analysis of an Industrial LS Interior PM Synchronous Motor," *2008 IEEE PES General meeting,* Pittsburgh, Pennsylvania, USA, pp. 1-6, July 2008

[16] M. Rahman, A. Osheiba, T. Radwan, "Synchronization process of line-start permanent magnet synchronous motor," *Electric Machines and Power Systems*, Taylor and Francis Ltd, vol. 25, pp. 577-592, 1997.

[17] J.F. Gieras, M. Wing, "Permanent magnet motor technology," Marcel Dekker Inc. New York, 2002.

[18] D. Stoia, M. Cernat, K. Hameyer, Dr. Ban, "Line-Start Permanent Magnet Synchronous Motors Analysis and Design", *EDPE 2009*, Dubrovnik, Croatia, , paper T02-014, Oct. 2009.

[19] T. Modeer, "Modelling and testing of Line Start Permanent Magnet Motors", Licentiate thesis, Royal Institute of Technology (KTH), Stockholm, Sweden, August 2007.